Article

Cell Stem Cell

Dual SMAD Signaling Inhibition Enables Long-Term Expansion of Diverse Epithelial Basal Cells

Graphical Abstract

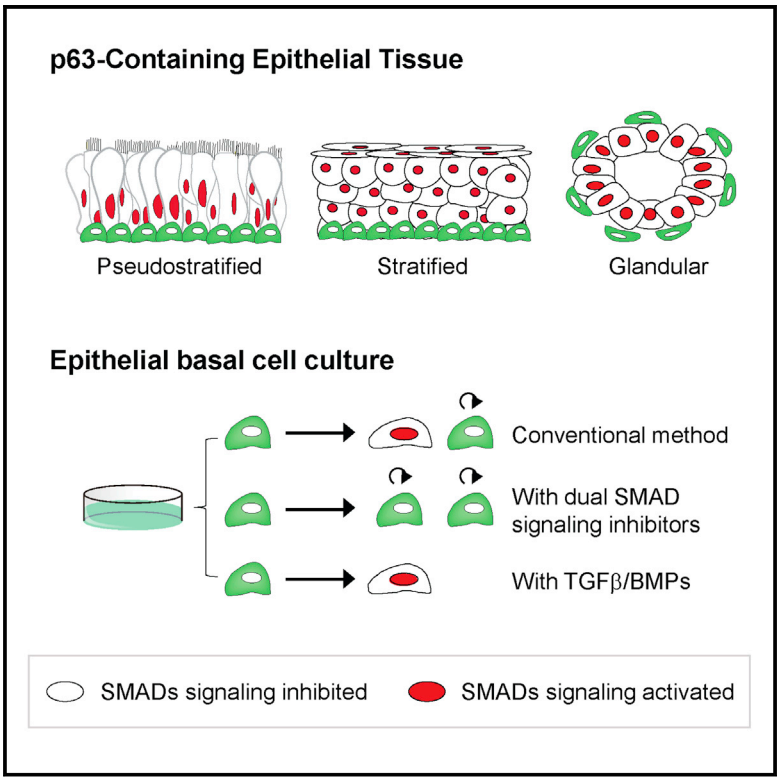

Authors

Hongmei Mou, Vladimir Vinarsky, Purushothama Rao Tata, ..., John F. Engelhardt, Ya-Chieh Hsu, Jayaraj Rajagopal

Correspondence

jrajagopal@partners.org

In Brief

Mou et al. show that small-molecule-mediated SMAD signaling inhibition allows prolonged feeder-free culture of diverse functional epithelial basal stem cells in a 2D format. This methodology provides a facile patient-specific epithelial disease modeling platform, as shown by the expansion of airway epithelium from non-invasively obtained specimens from cystic fibrosis patients.

Highlights

- SMAD activity is active in suprabasal cells but is weaker in basal epithelial cells
- SMAD signaling activity correlates with mucociliary differentiation in the airway
- Dual TGFβ/BMP inhibition prevents spontaneous differentiation in culture
- Dual TGFβ/BMP inhibition allows prolonged culture of diverse epithelial basal cells

Mou et al., 2016, Cell Stem Cell *19*, 217–231
August 4, 2016
http://dx.doi.org/10.1016/j.stem.2016.05.012

Cell Stem Cell
Article

Dual SMAD Signaling Inhibition Enables Long-Term Expansion of Diverse Epithelial Basal Cells

Hongmei Mou,[1,2,3] Vladimir Vinarsky,[1,2,4] Purushothama Rao Tata,[1,2] Karissa Brazauskas,[1,3] Soon H. Choi,[5] Adrianne K. Crooke,[5] Bing Zhang,[6] George M. Solomon,[7,10] Brett Turner,[8] Hermann Bihler,[11] Jan Harrington,[11] Allen Lapey,[3] Colleen Channick,[4] Colleen Keyes,[4] Adam Freund,[12] Steven Artandi,[12] Martin Mense,[11] Steven Rowe,[7,8,9,10] John F. Engelhardt,[5] Ya-Chieh Hsu,[6] and Jayaraj Rajagopal[1,2,3,4,13,*]
[1]Center for Regenerative Medicine, Massachusetts General Hospital, 185 Cambridge Street, Boston, MA 02114, USA
[2]Harvard Stem Cell Institute, Cambridge, MA 02138, USA
[3]Division of Pediatric Pulmonary Medicine, Massachusetts General Hospital for Children, Boston, MA 02114, USA
[4]Division of Pulmonary and Critical Care Medicine, Department of Internal Medicine, Massachusetts General Hospital, Boston, MA 02114, USA
[5]Department of Anatomy and Cell Biology, College of Medicine, University of Iowa, Iowa City, IA 52242, USA
[6]Department of Stem Cell and Regenerative Biology, Harvard University and Harvard Stem Cell Institute, 7 Divinity Avenue, Cambridge, MA 02138, USA
[7]Department of Medicine, University of Alabama at Birmingham, Birmingham, AL 35233, USA
[8]Department of Pediatrics, University of Alabama at Birmingham, Birmingham, AL 35233, USA
[9]Department of Cell, Developmental, and Integrative Biology, University of Alabama at Birmingham, AL 35294, USA
[10]Gregory Fleming James Cystic Fibrosis Research Center, University of Alabama at Birmingham, Birmingham, AL 35233, USA
[11]CFFT Lab, Cystic Fibrosis Foundation Therapeutics, Lexington, MA 01730, USA
[12]Departments of Medicine and Biochemistry, Stanford University, Stanford, CA 94305, USA
[13]Division of Otology and Laryngology, Massachusetts Eye and Ear, Boston, MA 02114, USA
*Correspondence: jrajagopal@partners.org
http://dx.doi.org/10.1016/j.stem.2016.05.012

SUMMARY

Functional modeling of many adult epithelia is limited by the difficulty in maintaining relevant stem cell populations in culture. Here, we show that dual inhibition of SMAD signaling pathways enables robust expansion of primary epithelial basal cell populations. We find that TGFβ/BMP/SMAD pathway signaling is strongly activated in luminal and suprabasal cells of several epithelia, but suppressed in p63+ basal cells. In airway epithelium, SMAD signaling promotes differentiation, and its inhibition leads to stem cell hyperplasia. Using dual SMAD signaling inhibition in a feeder-free culture system, we have been able to expand airway basal stem cells from multiple species. Expanded cells can produce functional airway epithelium physiologically responsive to clinically relevant drugs, such as CFTR modulators. This approach is effective for the clonal expansion of single human cells and for basal cell populations from epithelial tissues from all three germ layers and therefore may be broadly applicable for modeling of epithelia.

INTRODUCTION

Many epithelia are maintained by the regenerative capacity of adult stem cells. In stratified epithelia, basement membrane-resident p63$^+$ basal cells can self-renew and often act as stem cells that give rise to differentiated progeny (Van Keymeulen and Blanpain, 2012; Melino et al., 2015; Mills et al., 1999; Yang et al., 1999). In some instances, adult basal cells function as unipotent stem cells (Choi et al., 2012; Van Keymeulen et al., 2011), although these basal cells demonstrate a bipotent stem cell plasticity on transplantation (Van Keymeulen et al., 2011; Prater et al., 2014). Epithelial stem cell culture relying on co-culture with irradiated fibroblasts was pioneered by Rheinwald and Green (1975) and remains the standard method for long-term expansion of human keratinocytes. The use of Rho-associated protein kinase (ROCK) inhibition has further improved epithelial culture systems (Liu et al., 2012) and has been recently used to culture many organ-specific progenitor cells (Wang et al., 2015).

Despite these remarkable achievements, the prolonged expansion of adult epithelial stem cells remains challenging, and for many stratified and pseudostratified tissues there are no adequate culture systems and, importantly, no methodology to clone cells. Furthermore, feeders, as a contaminating cell population, may interfere with the mechanistic interpretation of the effects of genetic and pharmacologic manipulation. Organoid culture models offer an alternative to fibroblast co-culture systems allowing stem cells from many organs to be propagated (Barcellos-Hoff et al., 1989; Rock et al., 2009; Sato et al., 2009; Tadokoro et al., 2016; Yin et al., 2014). However, after decades of epithelial stem cell culture research, the ability to expand and manipulate pure adult stratified and pseudostratified epithelial stem cells remains limited.

The transforming growth factor-β (TGFβ) superfamily signaling has been implicated in regulating hematopoietic, hair follicle, melanocyte stem cell, and neural stem cell quiescence and activation (Genander et al., 2014; Kandasamy et al., 2014; Kobielak et al., 2007; Mira et al., 2010; Nishimura et al., 2010; Oshimori and Fuchs, 2012; Yamazaki et al., 2009). Additionally, BMP and

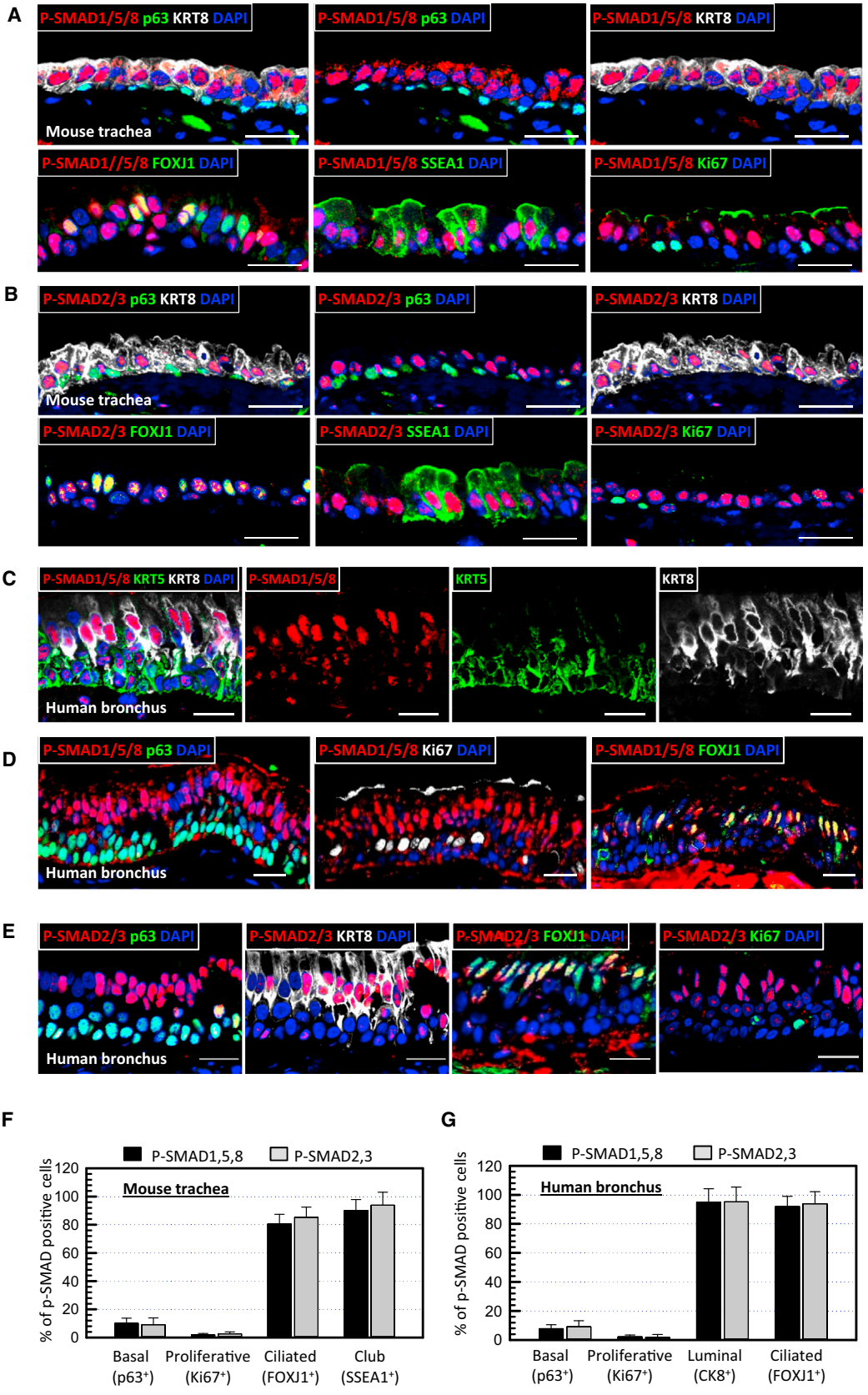

(legend on next page)

TGFβ signaling balances stem cell proliferation, differentiation, and reversible cell-cycle exit and thereby regulates the maintenance and dynamic behavior of normal reservoirs of stem cells capable of responding to tissue injury (Guasch et al., 2007; He et al., 2004; Kobielak et al., 2007; Oshimori and Fuchs, 2012). Indeed, BMP/TGFβ signaling antagonists have been used to facilitate the colon and mouse tracheal organoid culture (Sato et al., 2009; Tadokoro et al., 2016).

Given their roles in diverse stem cell systems, we assessed the role of BMP and TGFβ signaling in epithelia at large. We demonstrate that BMP and TGFβ signaling activity is relatively suppressed in $p63^+$ basal cells, but is highly active in luminal and suprabasal cells, which can represent either differentiated epithelial cells or unipotent non-basal progenitor cells (Choi et al., 2012; Van Keymeulen et al., 2011). We have exploited the use of dual SMAD signaling inhibition to overcome the growth arrest and differentiation encountered in the culture of primary adult basal cells. As a result, expanded murine and human cells maintain their ability to differentiate into functional tissues. Thus, we describe a culture system that may allow for the generation of non-invasive clinically relevant disease models across many organ systems. Additionally, the methodology allows for cloning human stem cells. This, in turn, provides the key to reproducibly developing clonally derived, genetically modified human epithelia. Airway epithelia derived in this manner do lose some of their physiologic properties over time, despite preserved cell differentiation. Future work will be needed to resolve this limitation.

RESULTS

SMAD Signaling Is Highly Active in the Luminal Cells of the Airway Epithelium

We used the mouse trachea as a model system to understand how TGFβ/BMP/SMAD signaling regulates basal stem cell behavior. The mouse trachea contains $p63^+$/$KRT5^+$ basal stem cells, which can self-renew and give rise to luminal ($KRT8^+$) secretory club cells and ciliated cells (Rock et al., 2009). Staining for both p-SMAD1/5/8 and p-SMAD2/3 (indicators of BMP and TGFβ signaling activity, respectively) was strongly positive in $KRT8^+$ luminal cells (Figures 1A and 1B). In contrast, $p63^+$ basal stem cells displayed weak or negative p-SMAD protein expression (Figures 1A and 1B). Furthermore, co-staining of p-SMAD with lineage-specific makers revealed that 92% ± 8% of $FOXJ1^+$ ciliated cells and 88% ± 7% of $SSEA1^+$ secretory cells were positive for p-SMAD1/5/8, while 94% ± 10% of ciliated cells and 93% ± 9% of secretory cells were positive for p-SMAD2/3 (Figure 1F), reflecting the dual activation of BMP and TGFβ signaling in luminal epithelia. In $p63^+$ basal stem cells, while the vast majority of cells were negative for p-SMAD, a small fraction of $p63^+$ cells were clearly positive for p-SMAD1/5/8 (9% ± 4%) and p-SMAD2/3 (10% ± 4%) (Figure 1F). We speculated that this population represents differentiating basal cells. In fact, these $p63^+$p-$SMAD^{low}$ cells also expressed a low level of KRT8, consistent with the onset of differentiation. Nearly all $Ki67^+$ replicating cells were negative or only weakly positive for p-SMAD1/5/8 and p-SMAD2/3 (Figures 1F and 1G), suggesting an inverse relationship between proliferation and SMAD signaling activity. The p-SMAD1/5/8 and p-SMAD2/3 staining pattern in the human bronchus mimicked the pattern seen in the mouse trachea (Figures 1C–1E and 1G).

SMAD Signaling Is Highly Active in Luminal and Suprabasal Cells, but Is Suppressed in Basal Cells in Epithelial Tissues of All Three Germ Layers

Next, we examined p-SMAD status in diverse mouse epithelia developmentally derived from each of the three germ layers (Figure 2A), including ectoderm-derived (skin and mammary gland), endoderm-derived (vocal fold, esophagus, and prostate), and mesoderm-derived (epididymis) tissues. The epithelial tissues were either stratified squamous (skin, vocal fold, and esophagus) or pseudostratified (trachea, prostate, mammary gland, and epididymis). All of these epithelial tissues possess $p63^+$ basal cells and $p63^-$ luminal and suprabasal cells that are the progeny of basal cells (such as in skin, vocal fold, esophagus, airway, and epididymis) or that self-sustain (such as in mammary gland and prostate). We found that in all of these tissues, p-SMAD1/5/8 and p-SMAD2/3 proteins were largely absent or weakly positive in $p63^+$ basal cells and $Ki67^+$ replicative cells, but were strongly positive in the $p63^-$ luminal and suprabasal cells (Figures 2B–2G). This consistent staining pattern suggests that the TGFβ/BMP/SMAD signaling pathways play a common role in diverse epithelia.

Activation of SMAD Signaling Occurs in Differentiating Luminal Cells following Injury

Since p-SMAD expression was primarily present in the differentiated luminal cells of airway, we assessed whether the phosphorylation of SMAD is associated with the progression of luminal differentiation during the early course of regeneration after sulfur dioxide (SO_2) injury (Pardo-Saganta et al., 2015; Tata et al., 2013). We found that at 8 hours post-injury (8 hpi), the majority of $CK8^+$p-$SMAD^+$ luminal cells in the proximal airway were sloughed off or loosely attached to the trachea, leaving behind a single layer of $p63^+SMAD^-$ basal stem cells (Figures 3A, 3B, and S1A). At 24 hpi, we observed massive proliferation and expansion of basal cells (Figures S1B and S1C). These replicating cells, which were $p63^+$ but $KRT8^-$, were negative for p-SMAD (Figures 3A, 3B, and S1A–S1C). Recently, we have demonstrated that c-MYB-expressing basal cells and N2ICD-expressing basal cells start to segregate as early as 6 hr after SO_2 injury, are fully segregated by 24 hr post-injury, and differentiate into ciliated and secretory cells, respectively (Pardo-Saganta et al., 2015). This suggests that the

Figure 1. SMAD Signaling Is Active in Differentiated Cells, but Is Suppressed in Basal Stem Cells of the Airway Epithelium

(A and B) Co-staining of p-SMAD1/5/8 (A) or p-SMAD2/3 (B) with basal stem cell marker p63, differentiation maker KRT8, ciliated cell marker FOXJ1, club cell marker SSEA1, and proliferation marker Ki67 on mouse tracheal sections.

(C and D) Co-staining of p-SMAD1/5/8 with KRT5 and KRT8 (C) and with p63, FOXJ1, and Ki67 (D) on human bronchial sections.

(E) Co-staining of p-SMAD2/3 with p63, KRT8, FOXJ1, and Ki67 on human bronchial sections.

(F and G) Quantification of the percentage of p-SMAD1/5/8^+ and p-SMAD2/3^+ cells of the indicated cell types in mouse trachea (F) and human bronchus (G), n = 3. Scale bars, 20 μm.

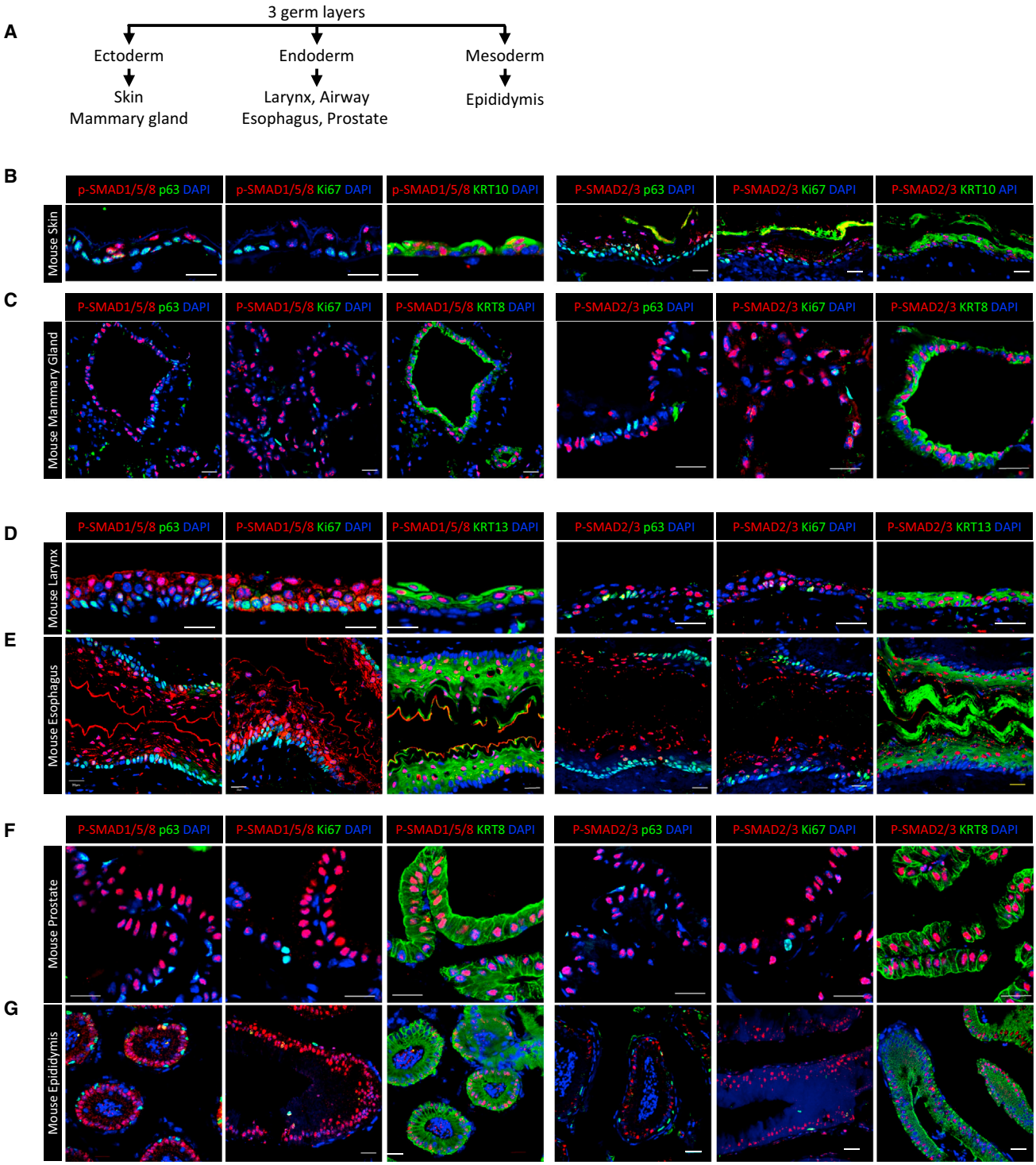

Figure 2. SMAD Signaling Is Active in Luminal and Suprabasal Cells but Is Suppressed in Basal Cells in Epithelial Tissues Derived from All Three Germ Layers

(A) Schematic of the analyzed p63^{+} basal cell-containing murine tissues derived from each germ layer.

(B–G) Co-staining of p-SMAD1/5/8 and p-SMAD2/3 with p63, Ki67, and a luminal and suprabasal marker KRT10 (B), KRT13 (D and E), or KRT8 (C, F, and G). Scale bar, 20 μm.

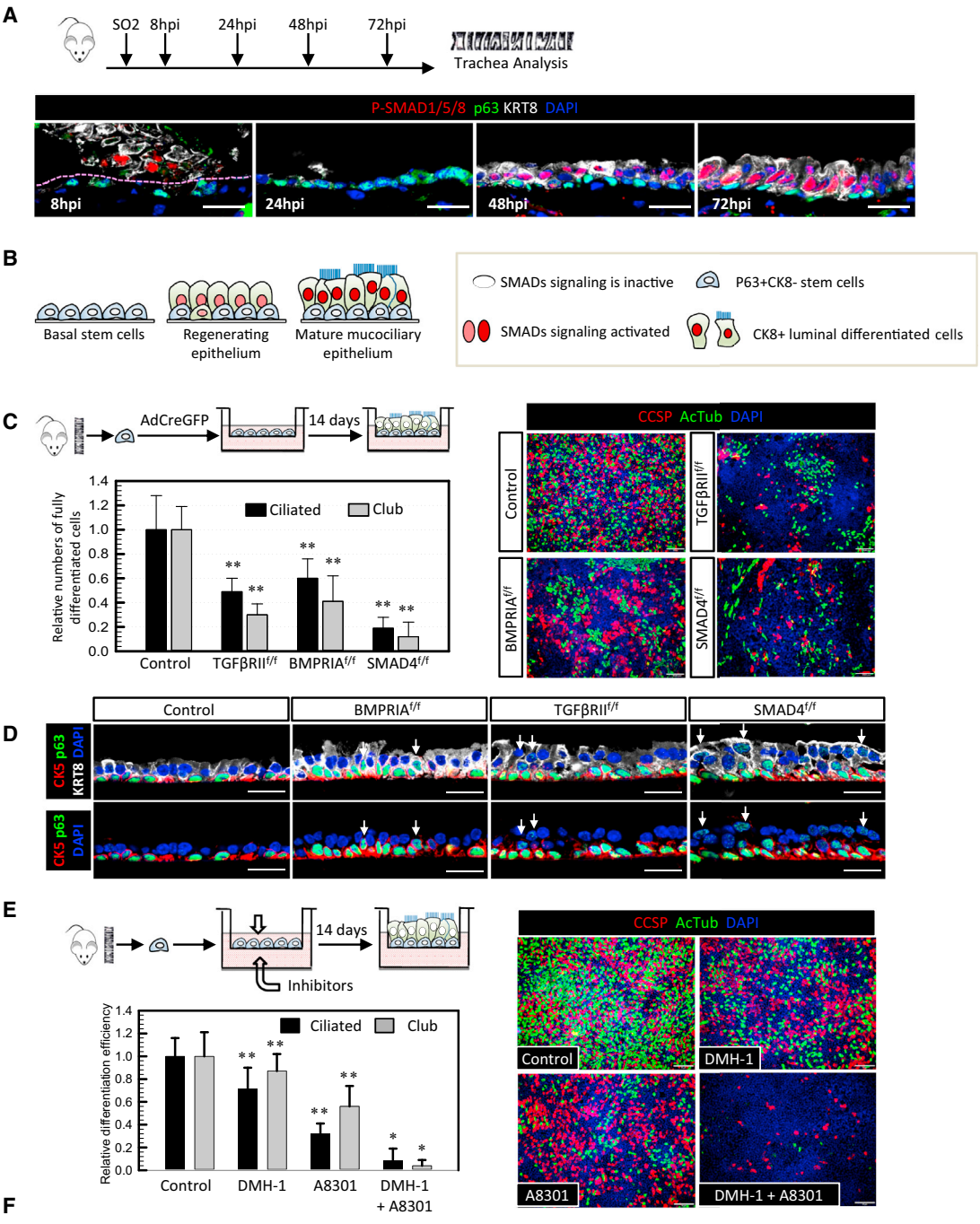

(legend on next page)

phosphorylation of SMAD is not involved in the cell-fate segregation of basal stem cells during regeneration, but rather is associated with the actual process of luminal cell formation, as marked by KRT8 expression. Indeed, luminal cells at 48 hpi began to express KRT8, coincident with increasing SMAD phosphorylation (Figures 3A, 3B, and S1A–S1C). By 72 hpi, the luminal cells further differentiated and began to express mature lineage-specific markers (Pardo-Saganta et al., 2015; Tata et al., 2013). Consistently, these luminal cells were now strongly positive for p-SMAD, while basal stem cells remained p-SMAD weak or negative (Figures 3A, 3B, and S1A–S1C).

We also examined SMAD phosphorylation during human airway stem cell mucociliary differentiation in air-liquid interface (ALI) culture (Figure S1D). 12 hr after ALI initiation (day 0.5), stem cells remained $p63^+KRT8^-$ and also negative for both p-SMAD1/5/8 and p-SMAD2/3 (Figure S1E). The following day (day 1.5), the cells began to stratify to form a differentiated second layer of $KRT8^+$p-$SMAD^+$ cells (Figure S1E). Some $p63^+$ cells were also positive for p-SMAD, perhaps suggesting that they are actively differentiating (Figure S1E). At days 2.5 and 3.5, more $KRT8^+$ p-$SMAD^+$ differentiated cells appeared, while the $p63^+$ basal cells were entirely p-SMAD negative or weak (Figure S1E). At day 13.5, when the luminal cells have already matured into ciliated cells and secretory cells, the phosphorylation of SMAD remained strongly positive in $KRT8^+$ luminal cells, but was largely absent or weak in $KRT5^+$ basal cells (Figure S1E). Thus, activation of SMAD signaling correlates with the appearance of $KRT8^+$ luminal cells in both mouse and human airway epithelial differentiation (Figure 3B). Furthermore, phosphorylation of SMAD is persistent in mature airway luminal cells.

Inhibition of SMAD Signaling Compromises Mucociliary Differentiation

Next, we tested whether SMAD signaling blockade inhibits mucociliary differentiation. We isolated GSIβ$4^+$$EpCAM^+$ murine airway basal stem cells (Zhao et al., 2014) from the trachea of wild-type, $BMPRIA^{f/f}$, $TGF\beta RII^{f/f}$, and $SMAD4^{f/f}$ mice and infected them with Adeno-CreGFP virus to delete the various signaling pathway components (Figures 3C and S1F). Mucociliary differentiation from the airway stem cells was performed using standard ALI culture. 2 weeks after initiation of ALI, a mature airway epithelium generated from WT-infected cells consisted of ciliated cells and secretory cells. Deletion of BMPRIA, TGFβRII, and SMAD4 resulted in significantly fewer differentiated cells (Figure 3C). Consistent with this finding, loss of BMPRIA, TGFβRII, and SMAD4 all resulted in airway epithelia with increased stratification and basal cells co-labeled with KRT8 (Figure 3D), suggesting that many basal stem cells have been trapped in a transitional state while differentiating into $KRT8^+$ luminal cells. Such differentiating cells are rarely found in the normal airway epithelium.

We also used BMP and TGFβ antagonists to examine mucociliary differentiation when BMP signaling or/and TGFβ signaling was blocked (Figure 3E). In controls, airway basal cells differentiated into airway epithelium with high efficiency after 2 weeks. In the presence of BMP antagonist (DMH-1) or TGFβ antagonist (A-83-01), fewer ciliated cells and club cells were generated. When both antagonists were used, the effect was more pronounced, with a >95% decrease in the production of differentiated cells (Figure 3E). Similarly, treatment with BMP and TGFβ antagonists induced basal cell hyperplasia with hyper-proliferative $KRT5^+/p63^+$ cells and transitional $KRT5^+/KRT8^+$ cells lining the luminal compartment (Figure 3F). Of note, ciliated cells and club cells did appear after prolonged ALI culture, even in the presence of the dual BMP/TGFβ inhibitors (Figure S1G). However, those ciliated and club cells that escaped inactivation were positive for p-SMAD staining (data not shown), supporting the tight association of differentiation with p-SMAD status. In summary, both genetic deletion and pharmacological inhibition abrogated efficient generation of secretory and ciliated cells, suggesting that SMAD activation promotes continued differentiation of early committed cells to terminal maturation.

Blockade of SMAD signaling also compromised mucociliary differentiation in human cells. Differentiation was significantly suppressed when SMAD4 expression was reduced (Figures S1H and S1I). Only a small number of ciliated cells with truncated cilia were detected and club cells were nearly absent after 2 weeks of ALI culture (Figure S1I). Again, prolonged differentiation was associated with some mucociliary differentiation (Figure 1J). Consistently, the epithelia derived from SMAD4 shRNA-treated cells have numerous $KRT5^+KRT8^+$ and $p63^+KRT8^+$ cells trapped in transitional state. We also observed more $Ki67^+$ cells in the SMAD4 small hairpin RNA (shRNA) epithelia compared to controls, suggesting that SMAD loss leads to increased proliferation (Figure S1J). These data indicate cross-species conservation in the requirement for SMAD signaling to execute epithelial differentiation.

Dual SMAD Signaling Inhibition Enables Long-Term Airway Stem Cell Expansion

Based on our observations that SMAD signaling is highly activated in non-cycling and differentiated luminal cells, we hypothesized that SMAD pathway inhibition would promote

Figure 3. Activation of SMAD Signaling Is Associated with Progressive Mucociliary Differentiation

(A) C57B6 mice were exposed to SO_2. At 8, 24, 48, and 72 hr post-SO_2 injury, the mice were sacrificed, and trachea were collected for co-staining of p-SMAD1/5/8 with p63 and KRT8. The dashed line separates the sloughed luminal cell debris from the attached residual basal cell layer.

(B) Schematic of SMAD signaling activation changes along the course of mucocilary differentiation.

(C) Tracheal stem cells isolated from wild-type, $BMPRIA^{f/f}$, $TGF\beta RII^{f/f}$, and $SMAD4^{f/f}$ mice were treated with Ad-Cre-GFP virus. The GFP^+ cells were sorted to purity 1–2 days post-infection. The cells were briefly expanded and then subjected to ALI differentiation. Left: quantification of ciliated cells and club cells in various conditions (mean ± SD, n = 3; $^{**}p \leq 0.001$). Right: whole-mount staining of $CCSP^+$ club cells and $AcTub^+$ ciliated cells on ALI membranes.

(D) Immunostaining for KRT5, p63, and KRT8 of transverse sections of ALI membranes. The arrows indicate representative transitional differentiating cells.

(E) Tracheal stem cells were isolated from WT mice and differentiated on ALI for 14 days. At day 0, 1 μM DMH-1 and/or 1 μM A-83-01 were added to the lower chamber and upper chamber (as a thin layer) to inhibit the corresponding SMAD signaling activity. Left: quantification of ciliated cells and club cells in various conditions (mean ± SD, n = 5; $^{**}p \leq 0.001$, $^{*}p \leq 0.01$). Right: whole-mount staining of $CCSP^+$ club cells and $AcTub^+$ ciliated cells on ALI membranes.

(F) Immunostaining for indicated markers of transverse sections of ALI membranes. The arrows indicate representative transitional differentiating cells.

Scale bars, 20 μm. See also Figure S1.

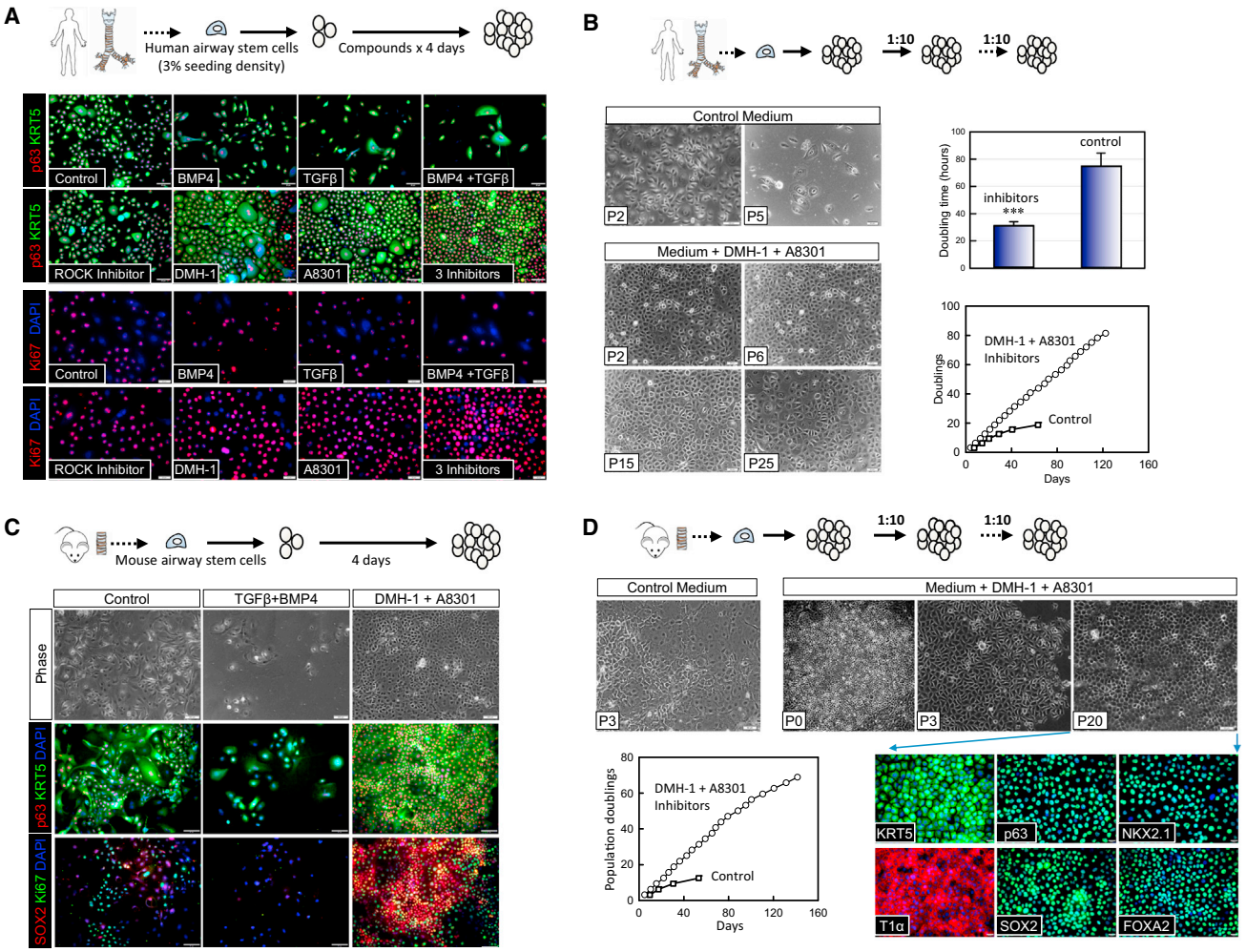

Figure 4. Dual SMAD Signaling Inhibition Facilitates Long-Term Expansion of Human Airway Stem Cells

(A) Human airway stem cells were expanded for 4 days in varying culture conditions. The cells were fixed and stained for p63, KRT5, and Ki67. Scale bar: upper two rows, 50 μm; lower two rows, 20 μm.

(B) Serial expansion of human airway stem cells in the control medium or the same medium with addition of TGFβ/BMP inhibitors. Left: phase-contrast images of the cells at various passages. Right: the average population doubling times (mean ± SD, n = 10; ***$p \leq 0.0001$) and a plot of number of doublings versus the culture times of the human airway stem cells cultured in various media (from one representative culture).

(C) Mouse tracheal stem cells were expanded for 4 days in varying culture conditions. The cells were fixed and stained for p63/KRT5 and Ki67/SOX2. Scale bar: upper, 100 μm, bottom, 50 μm.

(D) Serial expansion of mouse tracheal stem cells in the control medium or the same medium with addition of TGFβ/BMP inhibitors. Top: phase-contrast images of the mouse tracheal stem cells at various passages. Bottom: (left) the plot of number of doublings versus the culture times of mouse tracheal stem cells cultured in various conditions (from one representative culture) and (right) the staining of cell-fate markers on mouse tracheal stem cells at passage 20. Scale bar, 20 μm. See also Figures S2 and S5.

airway stem cell growth in vitro. Thus, we cultured human airway stem cells in various conditions (Figure 4A). Both BMP4 (50 ng/ml) and TGFβ (10 ng/ml) strongly suppressed cell growth. ROCK inhibitor (10 μM) alone modestly promoted cell expansion. However, both DMH-1 (1 μM) and A-83-01 (1 μM) greatly stimulated cell expansion. The three inhibitors together had the most profound effect (Figure 4A). The resultant cells were homogenous, small, and tightly packed, as is expected for stem cells. All cells were positive for KRT5 and p63, and >85% of cells were positive for Ki67 (Figure 4A). We also examined commonly used SMAD signaling inhibitors and found that they all similarly promoted cell growth (Figures S2A and S2B). Furthermore, we tested multiple previously reported culture media, including BEGM (Fulcher et al., 2005) and HTEK (You and Brody, 2013) (Figure S2C). Again, dual TGFβ/BMP inhibitors greatly enhanced cell proliferation in each of these media formulations. BMP and TGFβ are known to act through pathways other than the canonical SMAD pathway, including the MEK/MAPK, PI3K, and PKC-related cascades. Therefore, we tested the growth of human airway stem cells in the presence of their corresponding inhibitors. These compounds either had no effect or a detrimental effect on cell growth, suggesting that BMP and TGFβ inhibitors are indeed acting through SMAD (Figure S2D).

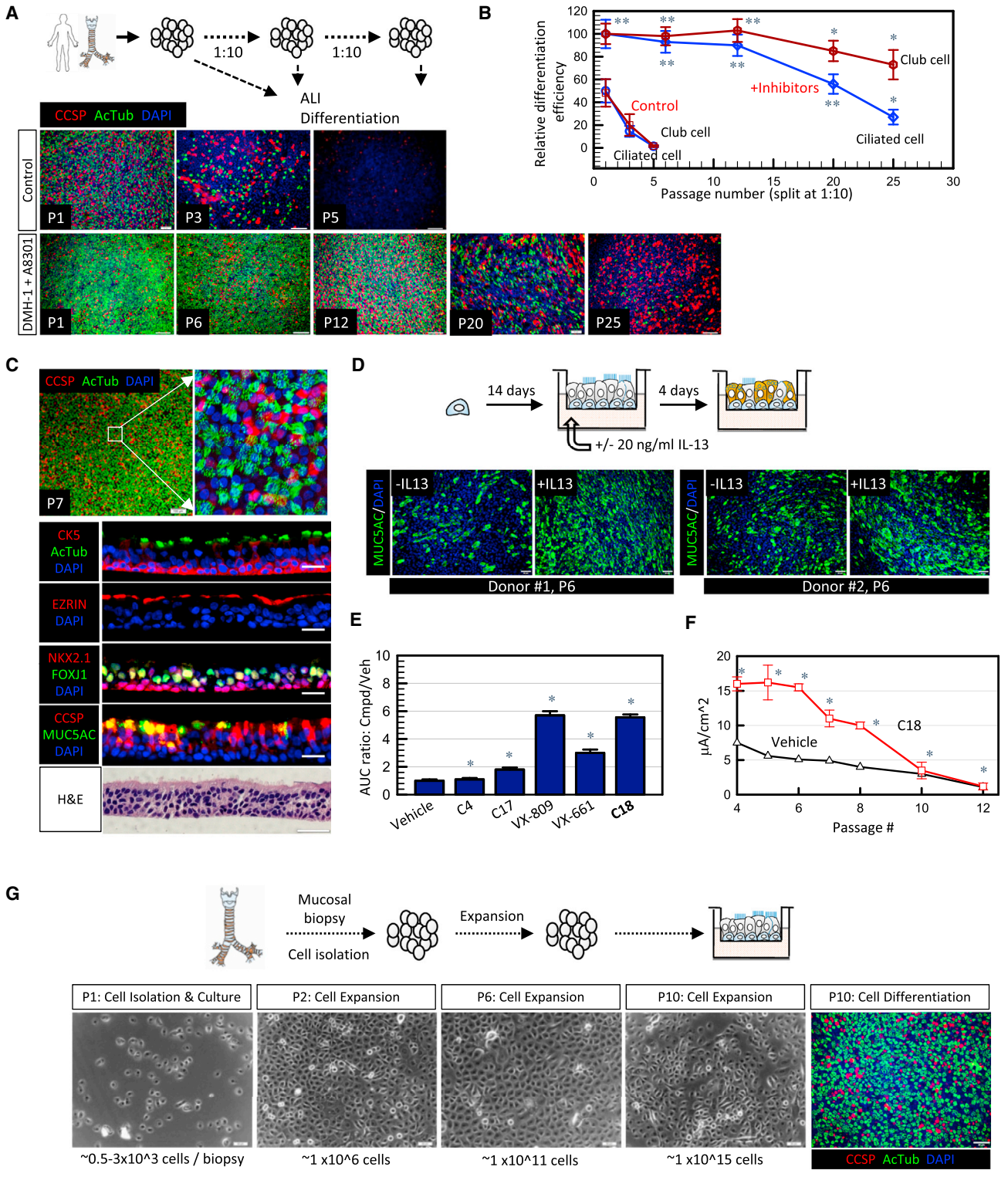

Figure 5. Expanded Airway Stem Cells Preserve the Potential to Differentiate into Functional Airway Epithelia

(A) Expanded human airway stem cells at different passages were differentiated on ALI for 16–20 days. The resultant membranes were fixed and stained for CCSP$^+$ club cells and AcTub$^+$ ciliated cells. Scale bar, 50 μm.

(B) Mucociliary differentiation efficiency at various passages (normalized to the efficiency of stem cell differentiation at P1 with TGFβ/BMP inhibitors) (mean ± SD, n = 3; **p ≤ 0.001, *p ≤ 0.01).

(C) Immunofluorescence staining for markers of differentiation using whole-mount (scale bar, 100 μm) and histology sections (scale bar, 20 μm) of P7 ALI cultures. Bottom, H&E staining of an ALI section (scale bar, 50 μm).

(legend continued on next page)

Next, we examined whether TGFβ/BMP inhibitors allow long-term expansion of human airway stem cells without fibroblast feeders. In the control medium, cells can be passaged only to P6 (~20 doublings at a 1:10 splitting ratio; Figure 4B). Cells grown in the presence of TGFβ or BMP4 did not expand beyond P1. With dual TGFβ/BMP inhibition, however, cells were able to expand to P18–P25 without a loss of replicative potential (~60–80 doublings, n = 9; Figure 4B). They divided faster and were more homogenous in size in contrast to controls (Figure 4B). Nearly all cells expressed the stem cell markers, as well as the transcription factors that define airway epithelial cell identity (Figures S2E and S2F). We did not detect KRT8 expression in the replicative $p63^+$ cells (data not shown), suggesting that dual TGFβ/BMP inhibitors completely blocked differentiation in 2D culture. Furthermore, TGFβ/BMP inhibition enabled single-cell cloning. Human airway stem cells from two healthy subjects were sorted as singles and individually expanded to test their proliferation potential and mucociliary differentiation capacity following cloning. All clones examined had full capacity for significant expansion and multipotent differentiation into ciliated cells and secretory cells (Figure S2G). We also assessed our ability to expand bronchial stem cells from two patients harboring the ΔF508/ΔF508-CFTR mutation (Figure S2H). With control medium, the cells reached an expected expansion barrier at P4 and P5, whereas in the presence of TGFβ/BMP inhibitors, these cell lines expanded to P12 and P17 and remained proliferative (Figure S2H). A similar effect was seen in mouse tracheal stem cell culture. Dual TGFβ/BMP inhibition strongly enhanced cell proliferation (Figure 4C). As a result, mouse tracheal stem cells can be expanded in a feeder-free culture system for a considerably larger number of passages than previously possible, while maintaining normal cell morphology and preserved stem cell identity (Figure 4D).

Loss of TGFβ signaling has been previously noted to lead to tumor formation in stratified epithelia (Guasch et al., 2007). To assess whether serial passaging is associated with tumorigenesis, we transplanted expanded human and mouse airway stem cells and human lung cancer A549 cells subcutaneously into NSG mice (Figure S2I). A549 cells robustly generated tumors in all cases after 2–8 weeks, with a latency determined by the number of injected cells (Figure S2I). We did not retrieve a single tissue outgrowth 8 months after injection of expanded human airway stem cells. Transplanted expanded mouse tracheal stem cells formed cystic structures, and immunofluorescence demonstrated that they were not tumors, but rather were comprised of differentiated ciliated and club cells (Figure S2J). The expanded cells remained genomically stable with no significant DNA alterations (no focal deletion, insertion, or aneuploidy) when compared to early passage HUES8 and HUES9 cells (Figure S2K). Furthermore, transcriptome analysis of airway stem cells at early and late passages did not reveal any changes in tumor-associated gene expression (Figure S2L; GSE80408).

Expanded Airway Stem Cells Maintain the Potential to Differentiate into Functional Airway Epithelia

We then tested the differentiation capacity of expanded human airway stem cells from early to late passages. The airway stem cells cultured in conventional medium can undergo efficient mucociliary differentiation only at early passages (Figure 5A). In contrast, human airway stem cells expanded in TGFβ/BMP inhibitors generated airway epithelium with extremely high efficiency through passage 12, representing approximately 40 doublings (Figures 5A and 5B). Mucociliary differentiation remained robust through later passages, although the efficiency gradually declined. Secretory cell production appeared to be more stable than ciliogenesis, as airway stem cells at P25 could still generate club cells (Figures 5A and 5B). Mouse airway stem cells also expanded and differentiated through passage 12 (Figures S3A and S3B).

Expanded airway stem cells not only maintained their differentiation potential but also the resultant epithelia preserved their physiologic functions. For example, differentiated airway epithelial cells responded to IL-13 by induction of $MUC5AC^+$ goblet cells in both human and murine epithelia (Figures 5D and S3C). Additionally, airway epithelia maintained the ion channel physiology expected for their CFTR genotypes. Epithelium derived from CFTR-ΔF508 stem cells (P4) effectively responded to benzamil, an inhibitor of the epithelial sodium channel (ENaC) (Figure S3D). CFTR chloride ion transport activity was readily stimulated following addition of the cyclic AMP (cAMP) agonist forskolin in combination with the VX770 potentiator. Pre-incubation with various CFTR-ΔF508 trafficking correctors (VX-809, VX-661, and C18) produced the anticipated salutary effects on chloride transport (Figures 5E and S3D). Chloride currents also appropriately diminished with the addition of the specific CFTR inhibitor, CFTRinh-172 (Figure S3D). Importantly, Na^+ currents and CFTR-mediated transmembrane Cl^--conductance declined over serial passages, in both normal and CFTR-ΔF508 epithelia, while transepithelial resistance was preserved (Figures 5F, S3E, and S3F).

Given the ability to expand airway stem cells, we proceeded to test whether we could generate a large number of patient-specific airway stem cells from small clinically relevant tissue biopsies. We performed mucosal biopsy with clinical biopsy forceps on discarded human trachea and bronchi. Thirty biopsies (ten biopsies from each of three donors) were taken throughout the proximal upper airways. We have obtained 100 to 2,000 viable airway basal stem cells per biopsy, and these cells robustly proliferated in the media with dual TGFβ/BMP inhibitor. Within 1 week, these cells expanded to nearly 1 million cells, and we could passage them at a 1:10 splitting ratio to $\sim 1 \times 10^{15}$ cells by P10 within 50 days. Differentiation analysis at P10 demonstrated that the cells were capable of forming polarized differentiated airway epithelia (Figure 5G).

(D) Staining for MUC5AC on human ALI cultures after treatment with IL-13. Scale bar, 50 μm.

(E) Area under the curve (AUC) ratios for CFTR correctors (Cmpd/Veh) measured on ΔF508/ΔF508 human bronchial ALI cultures (P4) (mean ± SD, n = 4; $^*p \leq 0.01$).

(F) Chloride current density gradually declines with increased passages. Up to passage 8, the response to C18 remains at ~3-fold the vehicle response; at P10 and P12 with the decrease in currents, compound effects can no longer be resolved (mean ± SD, n = 3; $^*p \leq 0.01$).

(G) The expansion and differentiation of airway stem cells isolated from human tracheal biopsies (n = 30).

See also Figures S3–S5.

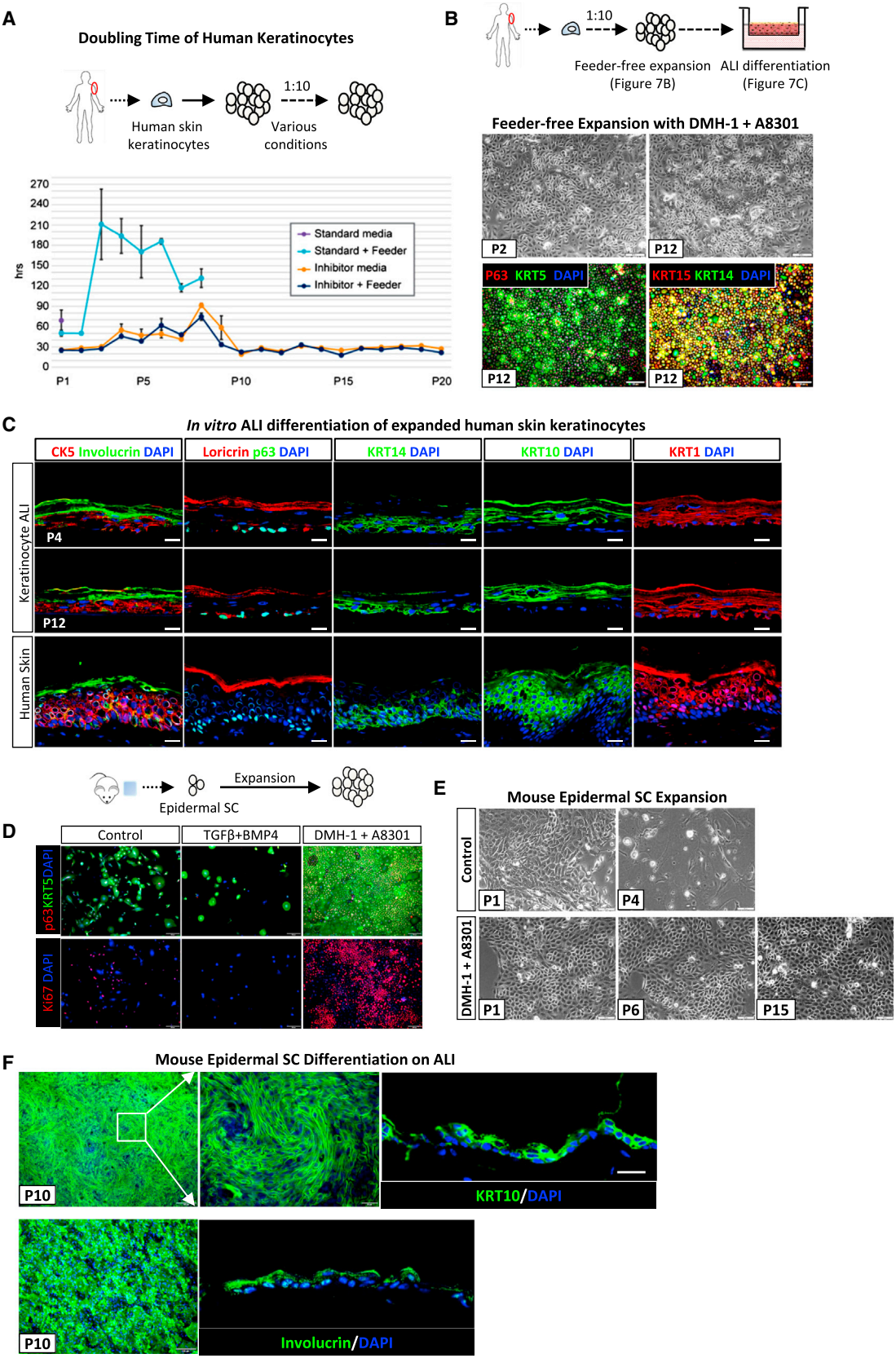

(legend on next page)

Bronchoscopy with transbronchial biopsy is an invasive procedure associated with complications. Thus, we tested the possibility to expand airway stem cells from bronchoalveolar lavage (BAL) or simply from an induced sputum. We demonstrate that by using media with dual TGFβ/BMP inhibitors, a small number of cells (<2,000 cells) from sputum or discarded BAL can be expanded to 10^{9-10} cells within a month and still remain proliferative (Figures S4A and S4B). Of patient samples, only one airway cell line was established from a total of five sputum samples. In the case of lavage, we produced three patient-specific lines out of three samples. The expanded cells were positive for the characteristic airway stem cell markers and capable of forming polarized mucociliary airway epithelia (Figures S4A and S4B). Thus, large amounts of airway epithelium can be obtained from patients entirely non-invasively. We also tested dual TGFβ/BMP inhibition in pig and ferret, species for which clinically relevant animal models of cystic fibrosis have been generated (Rogers et al., 2008; Sun et al., 2010). Our culture approach robustly expanded functional airway basal stem cells from the pig and the ferret (Figures S4C–S4E). Short-circuit current (Isc) measurements of differentiated ferret (P18) and pig epithelial cells (P7) demonstrate that, although the chloride current density diminished, the CFTR activity was still intact at the indicated passage numbers (Figure S4F).

SMAD Signaling Inhibition Promotes Stem Cell Self-Renewal by Inhibiting Differentiation, Independent of Telomere Crisis-Induced Cellular Senescence

Cellular senescence, defined as an irreversible cessation of cell division, has been proposed as the major obstacle preventing the long-term expansion of adult epithelial stem cells (Kiyono et al., 1998; Walters et al., 2013). However, we found that expression of the senescence marker p16ink4a is not correlated with growth arrest of human airway epithelial cells cultured in conventional medium (Figure S5A). On the other hand, we found that the majority of growth arrested cells are positive for KRT8, p-SMAD, and display a downregulation of p63 (Figure S5A). This staining pattern also occurs when early passage stem cells (P0–P1) were exposed to TGFβ and BMP4 (Figures S5B and S5C). Indeed, TGFβ and BMP4-exposed cells stopped proliferating, turned on KRT8, and did not alter p16ink4a expression (Figures S5B and S5C). Therefore, dual TGFβ/BMP inhibition contributes to sustained long-term stem cell expansion primarily by suppressing differentiation.

Telomere crisis has been suggested as the mechanism for growth arrest (Kiyono et al., 1998). Thus, we measured telomerase activity and telomere length in human airway stem cells during serial passaging. We did not detect any endogenous telomerase activity in human airway stem cells (Figure S5D), even at P0. As a result, telomeres gradually shortened during successive cell divisions (Figure S5E). In control cultures, proliferation of airway stem cells ceased after passage 5–6, a barrier that has been previously noted (Fulcher et al., 2005; Walters et al., 2013). However, telomere lengths of cells in control culture were similar to the telomere lengths of cells cultured in TGFβ/BMP inhibitors at the same passage (Figure S5E). Thus, the observed growth arrest in control medium was not caused by telomere shortening-induced crisis as we predicted before. Furthermore, dual TGFβ/BMP inhibition does not stabilize the telomeres, as the telomeres continued to shorten over passaging (Figure S5E). After P25–P30 (depending on the donor), airway stem cells abruptly stopped proliferating. This ultimate growth arrest precisely correlates with complete erosion of telomeres. Telomere length likely demarcates the intrinsic proliferative potential of a primary cell, while TGFβ/BMP dual inhibition facilitates stem cell self-renewal until eventually it reaches a bona fide telomere crisis-induced growth arrest. To test this hypothesis, we overexpressed hTERT in airway stem cells at early passage (P3) in order to stabilize the telomeres, and we saw a corresponding increase in the number of passages tolerated (Figures S5F and S5G). As predicted, cells with hTERT-stabilized telomeres remained acutely sensitive to differentiation induction triggered by withdrawal of the TGFβ/BMP inhibitors and the addition of TFGβ and BMP (Figure S5H). These data in aggregate demonstrate that precocious differentiation is the mechanism explaining the decreased cell replication and growth arrest that occurs in conventional cultures.

Next, we examined the effect of dual TGFβ/BMP inhibition on differentiated cells. Our laboratory has reported that airway club cells can undergo dedifferentiation into basal stem cells (Tata et al., 2013). By using CCSP-YFP club cells, we demonstrated that inhibition of SMAD signaling enhanced the dedifferentiation of club cells into $p63^{+}$ basal cells, while forced activation of SMAD signaling prevented it (Figures S5I–S5L).

Dual SMAD Signaling Inhibition Enables the In Vitro Expansion of Functional Keratinocytes

We hypothesized that dual SMAD signaling inhibition can be used to expand many diverse epithelial basal cell types. We first tested this hypothesis with epidermal keratinocytes as they historically have been the first extensively cultured basal stem cells (Rheinwald and Green, 1975). Our data indicated that human keratinocytes cannot be expanded without the use of feeder cells, consistent with the published literature (Rheinwald and Green, 1975, 1977) (Figure 6A). With feeder cells, keratinocytes formed holoclones and could be passaged for many generations

Figure 6. Dual SMAD Signaling Inhibition Enables Long-Term Expansion of Functional Keratinocytes

(A) Doubling time of adult human keratinocytes cultured in four different conditions: (1) standard media, (2) standard media + J2 feeder cells, (3) inhibitor media, and (4) inhibitor media + J2 feeder cells (mean ± SD, n = 3; $^{**}p \leq 0.001$).

(B) Phase-contrast images and marker staining of human keratinocytes at indicated passages expanded in a feeder-free mode in the medium containing TGFβ/BMP inhibitors. Scale bar, 100 μm.

(C) Section immunofluorescence of various basal and differentiation markers on ALI culture (P4 and P12) and on human skin. Scale bar, 20 μm.

(D) Isolated mouse keratinocytes were seeded at 3% cell density and expanded for 4 days in various culture conditions. The cells were then fixed and stained for p63, KRT5, and Ki67. Scale bar, 100 μm.

(E) Phase-contrast images of mouse skin keratinocytes at indicated passages. Scale bar, 50 μm.

(F) Differentiation of expanded mouse skin keratinocytes (P10) on ALI. The derived stratified epithelia were positive for KRT10 and involucrin.

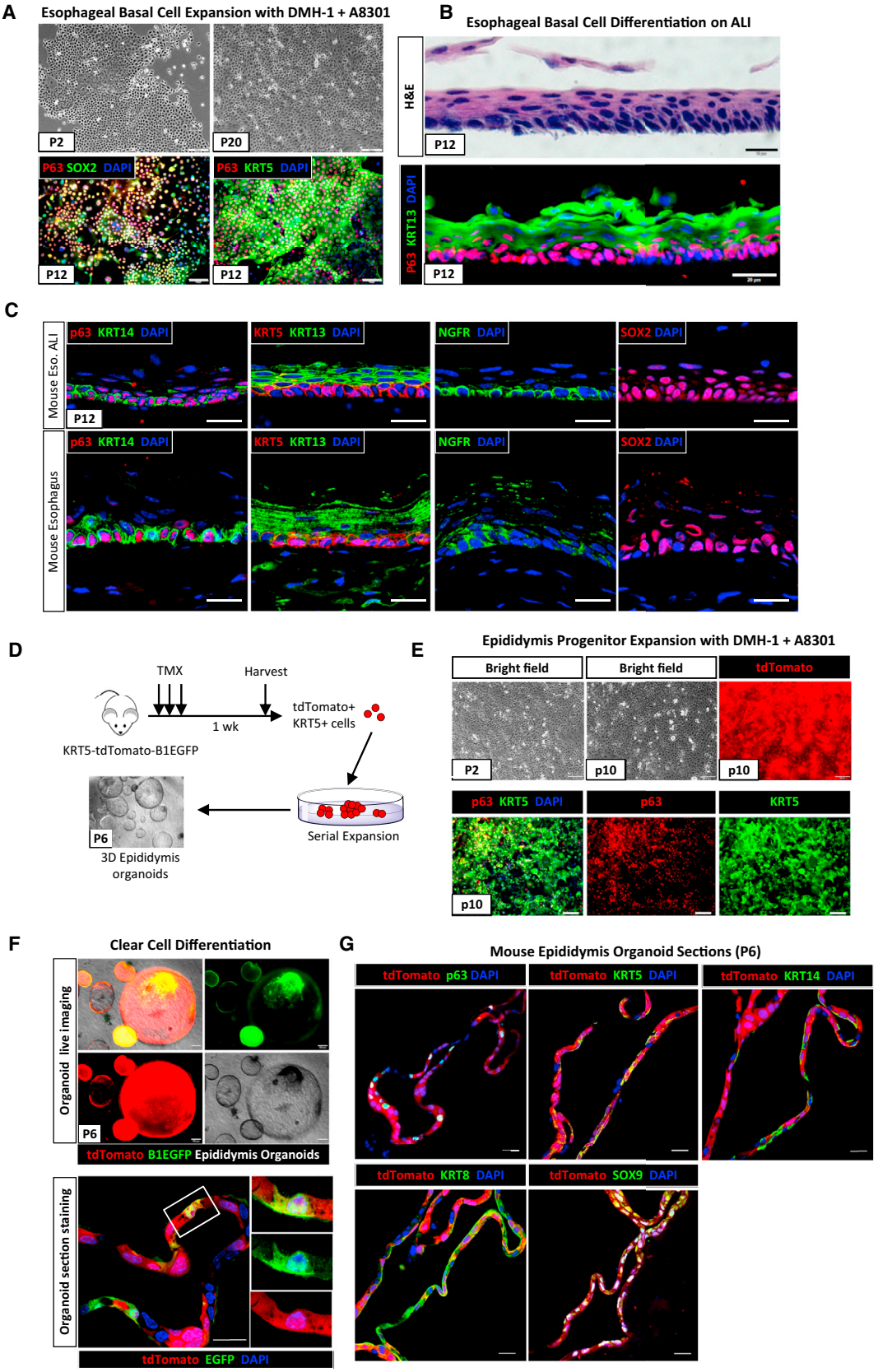

(legend on next page)

as previously described (Rheinwald and Green, 1977), but with the expected long doubling time (experiments were terminated at P8) (Figure 6A). In the presence of TGFβ/BMP inhibitors, keratinocyte growth was no longer dependent on feeder cells (Figure 6A). Indeed, the cells showed faster growth rates, with a 2- to 3-fold decrease in the population doubling time compared to growth on feeders. Interestingly, in the presence of TGFβ/BMP inhibitors, the addition of feeder cells did not further promote keratinocyte proliferation (Figure 6A). Human keratinocytes grown in inhibitor media were uniformly positive for typical stem cell markers (Figure 6B). When differentiated on ALI, expanded human keratinocytes generated stratified epithelial cells with the appropriate cellular architecture and markers akin to their in vivo counterparts (Figure 6C).

Mouse keratinocyte expansion also depends on a feeder layer at the start of the culture, although unlike human keratinocytes, mouse keratinocytes can be cultured off feeders after several generations. We cultured and expanded murine skin keratinocytes in feeder-free manner with and without TGFβ/BMP4, as well as with their inhibitors (Figures 6D and 6E). Murine skin keratinocytes failed to grow in the presence of TGFβ or BMP4. In control media, the cells grew slowly and could not be expanded to higher passages (Figures 6D and 6E). However, TGFβ/BMP inhibitors robustly stimulated cell proliferation and enabled prolonged cell expansion (Figures 6D and 6E). Similarly, the expanded mouse skin keratinocytes produced a stratified epithelium when differentiated on ALI (Figure 6F).

Dual SMAD Signaling Inhibition Enables In Vitro Expansion of a Diverse Set of Epithelial Basal Cells

In order to further explore the potential generalized use of dual SMAD signaling inhibition in promoting epithelial basal cell expansion, we isolated murine basal cells from representative epithelial tissues from each of the three germ layers. We demonstrate that epithelial basal cells isolated from esophagus (Figure 7A), epididymis (Figures 7D and 7E), larynx/vocal fold (Figures S6A and S6B), forestomach (Figures S6D and S6E), and mammary gland (Figures S7A and S7B) could be expanded to high passage numbers, while still maintaining their replicative potential, as well as normal cell morphology and appropriate stem cell markers.

The expanded cells also retained the capacity to differentiate efficiently. We demonstrate that expanded esophageal basal cells efficiently generated a stratified epithelium on transwell membranes (Figures 7B and 7C). The differentiated stratified esophageal epithelium had appropriate cellular morphology and markers, consistent with those of esophageal tissue (Figures 7B and 7C). Similarly, the expanded laryngeal basal cells and forestomach basal cells produced stratified epithelia when differentiated on ALI, and they possessed the same cellular architecture and marker expression as their corresponding tissues (Figures S6C and S6F).

Expanded epididymis basal cells and mammary basal cells efficiently generated organoids in Matrigel. Epididymis basal cells from a KRT5-tdTomato-B1EGFP mouse (V-ATPase B1 is a differentiated clear cell marker; V-ATPase B1-GFP is referred to as "B1EGFP") (Miller et al., 2005) generated organoids containing GFP^+ cells, indicating the presence of clear cells (Figure 7F). The epithelia were also positive for typical markers found in the epididymis tissue (Figures 7G and S7G). Furthermore, the expanded epididymis basal cells formed spheres after subcutaneous injection in vivo (Figures S7E and S7F). Tubular organoids contained a pseudostratified epididymal epithelium characterized by $KRT5^+$ basal cells and $KRT8^+$ luminal cells, as well as principal cells marked by AQP9 (Figure S7F). Similarly, derived mammospheres from expanded mammary basal cells possessed typical cellular architecture and marker expression characteristic of mammary tissue (Figures S7C and S7D). Taken together, we identified a method to expand epithelial basal cells from a diverse collection of murine tissues and demonstrated preserved differentiation potential of the expanded basal cells.

DISCUSSION

Dual SMAD signaling inhibition permits the expansion of adult epithelial basal cells from a wide array of organs and highlights a commonality of the role of the TGFβ/BMP/SMAD signaling pathway in regulating epithelial basal cell behavior. Prior cultures considered to have been arrested because of senescence likely failed due to unwanted differentiation. Interestingly, dedifferentiation can be enhanced using TGFβ/BMP/SMAD signaling inhibitors, demonstrating that the pathway has consistent effects on differentiation and dedifferentiation and implying that differentiation and dedifferentiation are mechanistically two sides of the same coin. Strictly speaking, TGFβ/BMP/SMAD signaling inhibition compromises terminal differentiation. A nearly identical phenotype has been reported following YAP overexpression in airway basal stem cells (Zhao et al., 2014). These converging phenotypes are no doubt related to the mechanisms governing specific steps of the differentiation cascade. We speculate that the effect of dual SMAD signaling inhibition reflects the presence of a highly evolutionarily conserved signaling network that regulates p63 and its associated pathways to maintain epithelial basal cell identity and prevent differentiation.

Figure 7. Dual SMAD Signaling Inhibition Enables In Vitro Expansion of a Diverse Set of Organ-Specific Basal Cells

(A) Phase-contrast images and marker staining of mouse esophageal basal cells at indicated passages expanded in the medium containing TGFβ/BMP4 inhibitors. Scale bar, 100 μm (phase-contrast images) and 50 μm (immunofluorescence).

(B and C) H&E (B) and immunofluorescence (B and C) of ALI culture sections derived from esophageal basal cells (P12) and of mouse esophageal. Scale bar, 20 μm.

(D) Schematic and example of organoid differentiation of expanded mouse epididymis basal cells isolated from KRT5-tdTomato-B1EGFP mouse.

(E) Phase-contrast images and immunofluorescence of mouse epididymis basal cells at indicated passages expanded with TGFβ/BMP4 inhibitors. Scale bar, 100 μm.

(F) Fluorescence images of tdTomato and EGFP in differentiated organoids from (D) (upper panels are whole-mount 3D organoids (scale bar, 100 μm) and bottom panels are sections of the organoids (scale bar, 20 μm).

(G) Co-immunofluorescence of indicated markers with tdTomato on epididymis organoid sections. Scale bar, 20 μm.

See also Figures S6 and S7.

A single bronchoscopic lavage reproducibly generates the substrate for large quantities of airway epithelium. Remarkably, in 1 out of 5 cases, even sputum from CF patients was sufficient to generate diseased airway epithelium. If methods for sputum induction could be improved, this would represent the least invasive way to generate human stem cells in any existing organ. It is possible that organs damaged in a disease process would be more likely to yield stem cells since more epithelial cell are being shed. Similar non-invasive methodologies might be used to generate epithelia from the secretions of many other epithelial organs, so that the collection of human stem cells is less invasive than a routine blood test. For now, a bronchoscopic lavage or nasal brushing is required for a perfect yield, but, again, sinus lavage is likely sufficient to reproducibly yield large quantities of respiratory epithelium for study. Furthermore, we hope our newfound ability to clone human epithelial stem cells will enable the creation of reproducible human model systems that can be genetically modified.

Despite these promising results, it is necessary to recognize that in vitro culture still has limitations. For example, we observed that expanded human airway stem cell-derived epithelia gradually lose CFTR-mediated chloride and ENaC-mediated sodium conductance, but, interestingly, they do maintain transepithelial resistance and differentiation potential. In fact, several studies (Pavlov et al., 2014; Staruschenko et al., 2004) have demonstrated the negative effect of ROCK inhibitor Y-27632 and EGF on ENaC activity, which may explain the gradual decrease in ENaC-mediated sodium conductance in cells expanded in the presence of Y-27632 and EGF. Partial loss of cellular physiological function in in vitro culture systems may be more common than previously recognized and may be tissue and function specific. For example, airway epithelium appears to preserve club cell differentiation potential longer than ciliated cell differentiation potential, and CFTR-mediated function appears to be lost even faster than ciliated cell differentiation. We speculate that the mechanisms involved in the differential deterioration of different physiologic cellular functions at distinct passage numbers are likely epigenetic. If so, epigenetic modulation is likely to be of value.

EXPERIMENTAL PROCEDURES

Human and Mouse Airway Stem Cell Isolation and Serial Expansion

Human and mouse airway stem cells were isolated from fresh human tissues (trachea and mainstem bronchi) or mouse trachea (Zhao et al., 2014). The cells were cultured in the medium either alone or with 5–10 μM ROCKi, 0.5–1 μM A-83-01, 0.5–1 μM DMH-1, and 1 μM CHIR99021 separately or in various combinations on plates pre-coated with laminin-enriched 804G-conditioned medium. To split the cell cultures, the cells were dissociated with trypsin and reseeded at a 1:10 ratio (see the Supplemental Experimental Procedures for detailed isolation and culture method).

Mucociliary Differentiation on Air-Liquid Interface Culture

Human or mouse airway stem cell cultures were seeded onto 0.4-μm transwell membranes pre-coated with 804G-conditioned medium with a density of >6,000 cells/mm^2. After cell attachment for >12 hr, excess cells were removed and the medium was replaced with complete Pneumacult-ALI medium (StemCell Technology, cat. 05001) or vertex ALI medium (Neuberger et al., 2011) filling both the upper and lower chambers. The next day, ALI medium was added only in the lower chamber to initiate airway-liquid interface. Then the medium was changed daily until differentiation was well established. Ciliogenesis was monitored by inverted-phase microscopy for beating cilia. We cultured ALI for 14–16 days as a standard protocol. For some experiments, we extended the ALI culture for 4–5 weeks.

TSA-Based Immunofluorescence

All Phospho-SMAD staining was performed using tyramide signal amplification (TSA) method. After antigen retrieval, the slides were incubated with diluted primary antibody at 4°C overnight. Of note, the primary antibodies used in TSA staining were usually diluted at 1:5,000–1:10,000. The next day, the slides were incubated with HRP-conjugated antibody at 1:2,000 for 1–2 hr and then with TSA working solution (1:100 dilution) for 15 min, followed by incubation with Streptavidin-594 diluted at 1:200 for 10–30 min (see the Supplemental Experimental Procedures for detailed staining method).

SUPPLEMENTAL INFORMATION

Supplemental Information includes Supplemental Experimental Procedures and seven figures and can be found with this article online at http://dx.doi.org/10.1016/j.stem.2016.05.012.

AUTHOR CONTRIBUTIONS

H.M. designed and conducted the experiments and wrote the manuscript. V.V. implemented the human cell and tissue protocols. V.V., P.R.T, and K.B. assisted in the mouse work. S.H.C., A.K.C., and J.F.E. performed the ferret and pig tracheal stem cells culture and analysis. B.Z. and Y.-C.H. performed the human keratinocyte culture and analysis. G.M.S., B.T., J.H, H.B., M.M., and S.R. conducted the CFTR physiological function analysis. A.L., C.C., and C.K. collected sputum and BAL. A.F. and S.A. performed the TRAP and TRF. V.V., P.R.T., and J.R. edited the manuscript. J.R. oversaw the work and co-wrote the manuscript.

ACKNOWLEDGMENTS

J.R. is a New York Stem Cell Foundation Robertson Investigator and a Maroni Research Scholar at MGH. We thank Marina Mazur (the University of Alabama at Birmingham) for assistance with cell culture and the entire J.R. laboratory for constructive comments. This research was supported by grants from the NIH (R01HL116756 and R01HL118185 to J.R.; DK047967 and HL051670 to J.F.E; K08HL124298 to V.V.; T32HL087735 to H.M.; K99HL127181 to P.R.T.; R00 AR063127 to Y.-C.H.), the Cystic Fibrosis Foundation (RAJAGO12G0 and RAJAGO12I0 to J.R.), and the Smith Family Awards and March of Dimes Basil O'Connor Starter Scholar Awards (to Y.-C.H.).

Received: March 11, 2016
Revised: April 30, 2016
Accepted: May 13, 2016
Published: June 16, 2016

REFERENCES

Barcellos-Hoff, M.H., Aggeler, J., Ram, T.G., and Bissell, M.J. (1989). Functional differentiation and alveolar morphogenesis of primary mammary cultures on reconstituted basement membrane. Development *105*, 223–235.

Choi, N., Zhang, B., Zhang, L., Ittmann, M., and Xin, L. (2012). Adult murine prostate basal and luminal cells are self-sustained lineages that can both serve as targets for prostate cancer initiation. Cancer Cell *21*, 253–265.

Fulcher, M.L., Gabriel, S., Burns, K.A., Yankaskas, J.R., and Randell, S.H. (2005). Well-differentiated human airway epithelial cell cultures. Methods Mol. Med. *107*, 183–206.

Genander, M., Cook, P.J., Ramsköld, D., Keyes, B.E., Mertz, A.F., Sandberg, R., and Fuchs, E. (2014). BMP signaling and its pSMAD1/5 target genes differentially regulate hair follicle stem cell lineages. Cell Stem Cell *15*, 619–633.

Guasch, G., Schober, M., Pasolli, H.A., Conn, E.B., Polak, L., and Fuchs, E. (2007). Loss of TGFbeta signaling destabilizes homeostasis and promotes squamous cell carcinomas in stratified epithelia. Cancer Cell *12*, 313–327.

He, X.C., Zhang, J., Tong, W.-G., Tawfik, O., Ross, J., Scoville, D.H., Tian, Q., Zeng, X., He, X., Wiedemann, L.M., et al. (2004). BMP signaling inhibits intestinal stem cell self-renewal through suppression of Wnt-beta-catenin signaling. Nat. Genet. *36*, 1117–1121.

Kandasamy, M., Lehner, B., Kraus, S., Sander, P.R., Marschallinger, J., Rivera, F.J., Trümbach, D., Ueberham, U., Reitsamer, H.A., Strauss, O., et al. (2014). TGF-beta signalling in the adult neurogenic niche promotes stem cell quiescence as well as generation of new neurons. J. Cell. Mol. Med. *18*, 1444–1459.

Kiyono, T., Foster, S.A., Koop, J.I., McDougall, J.K., Galloway, D.A., and Klingelhutz, A.J. (1998). Both Rb/p16INK4a inactivation and telomerase activity are required to immortalize human epithelial cells. Nature *396*, 84–88.

Kobielak, K., Stokes, N., de la Cruz, J., Polak, L., and Fuchs, E. (2007). Loss of a quiescent niche but not follicle stem cells in the absence of bone morphogenetic protein signaling. Proc. Natl. Acad. Sci. USA *104*, 10063–10068.

Liu, X., Ory, V., Chapman, S., Yuan, H., Albanese, C., Kallakury, B., Timofeeva, O.A., Nealon, C., Dakic, A., Simic, V., et al. (2012). ROCK inhibitor and feeder cells induce the conditional reprogramming of epithelial cells. Am. J. Pathol. *180*, 599–607.

Melino, G., Memmi, E.M., Pelicci, P.G., and Bernassola, F. (2015). Maintaining epithelial stemness with p63. Sci. Signal. *8*, re9.

Miller, R.L., Zhang, P., Smith, M., Beaulieu, V., Paunescu, T.G., Brown, D., Breton, S., and Nelson, R.D. (2005). V-ATPase B1-subunit promoter drives expression of EGFP in intercalated cells of kidney, clear cells of epididymis and airway cells of lung in transgenic mice. Am. J. Physiol. Cell Physiol. *288*, C1134–C1144.

Mills, A.A., Zheng, B., Wang, X.J., Vogel, H., Roop, D.R., and Bradley, A. (1999). p63 is a p53 homologue required for limb and epidermal morphogenesis. Nature *398*, 708–713.

Mira, H., Andreu, Z., Suh, H., Lie, D.C., Jessberger, S., Consiglio, A., San Emeterio, J., Hortigüela, R., Marqués-Torrejón, M.A., Nakashima, K., et al. (2010). Signaling through BMPR-IA regulates quiescence and long-term activity of neural stem cells in the adult hippocampus. Cell Stem Cell *7*, 78–89.

Neuberger, T., Burton, B., Clark, H., and Van Goor, F. (2011). Use of primary cultures of human bronchial epithelial cells isolated from cystic fibrosis patients for the pre-clinical testing of CFTR modulators. Methods Mol. Biol. *741*, 39–54.

Nishimura, E.K., Suzuki, M., Igras, V., Du, J., Lonning, S., Miyachi, Y., Roes, J., Beermann, F., and Fisher, D.E. (2010). Key roles for transforming growth factor beta in melanocyte stem cell maintenance. Cell Stem Cell *6*, 130–140.

Oshimori, N., and Fuchs, E. (2012). Paracrine TGF-β signaling counterbalances BMP-mediated repression in hair follicle stem cell activation. Cell Stem Cell *10*, 63–75.

Pardo-Saganta, A., Law, B.M., Tata, P.R., Villoria, J., Saez, B., Mou, H., Zhao, R., and Rajagopal, J. (2015). Injury induces direct lineage segregation of functionally distinct airway basal stem/progenitor cell subpopulations. Cell Stem Cell *16*, 184–197.

Pavlov, T.S., Levchenko, V., and Staruschenko, A. (2014). Role of Rho GDP dissociation inhibitor α in control of epithelial sodium channel (ENaC)-mediated sodium reabsorption. J. Biol. Chem. *289*, 28651–28659.

Prater, M.D., Petit, V., Alasdair Russell, I., Giraddi, R.R., Shehata, M., Menon, S., Schulte, R., Kalajzic, I., Rath, N., Olson, M.F., et al. (2014). Mammary stem cells have myoepithelial cell properties. Nat. Cell Biol. *16*, 942–950.

Rheinwald, J.G., and Green, H. (1975). Serial cultivation of strains of human epidermal keratinocytes: the formation of keratinizing colonies from single cells. Cell *6*, 331–343.

Rheinwald, J.G., and Green, H. (1977). Epidermal growth factor and the multiplication of cultured human epidermal keratinocytes. Nature *265*, 421–424.

Rock, J.R., Onaitis, M.W., Rawlins, E.L., Lu, Y., Clark, C.P., Xue, Y., Randell, S.H., and Hogan, B.L.M. (2009). Basal cells as stem cells of the mouse trachea and human airway epithelium. Proc. Natl. Acad. Sci. USA *106*, 12771–12775.

Rogers, C.S., Stoltz, D.A., Meyerholz, D.K., Ostedgaard, L.S., Rokhlina, T., Taft, P.J., Rogan, M.P., Pezzulo, A.A., Karp, P.H., Itani, O.A., et al. (2008). Disruption of the CFTR gene produces a model of cystic fibrosis in newborn pigs. Science *321*, 1837–1841.

Sato, T., Vries, R.G., Snippert, H.J., van de Wetering, M., Barker, N., Stange, D.E., van Es, J.H., Abo, A., Kujala, P., Peters, P.J., and Clevers, H. (2009). Single Lgr5 stem cells build crypt-villus structures in vitro without a mesenchymal niche. Nature *459*, 262–265.

Staruschenko, A., Nichols, A., Medina, J.L., Camacho, P., Zheleznova, N.N., and Stockand, J.D. (2004). Rho small GTPases activate the epithelial Na(+) channel. J. Biol. Chem. *279*, 49989–49994.

Sun, X., Sui, H., Fisher, J.T., Yan, Z., Liu, X., Cho, H.-J., Joo, N.S., Zhang, Y., Zhou, W., Yi, Y., et al. (2010). Disease phenotype of a ferret CFTR-knockout model of cystic fibrosis. J. Clin. Invest. *120*, 3149–3160.

Tadokoro, T., Gao, X., Hong, C.C., Hotten, D., and Hogan, B.L.M. (2016). BMP signaling and cellular dynamics during regeneration of airway epithelium from basal progenitors. Development *143*, 764–773.

Tata, P.R., Mou, H., Pardo-Saganta, A., Zhao, R., Prabhu, M., Law, B.M., Vinarsky, V., Cho, J.L., Breton, S., Sahay, A., et al. (2013). Dedifferentiation of committed epithelial cells into stem cells in vivo. Nature *503*, 218–223.

Van Keymeulen, A., and Blanpain, C. (2012). Tracing epithelial stem cells during development, homeostasis, and repair. J. Cell Biol. *197*, 575–584.

Van Keymeulen, A., Rocha, A.S., Ousset, M., Beck, B., Bouvencourt, G., Rock, J., Sharma, N., Dekoninck, S., and Blanpain, C. (2011). Distinct stem cells contribute to mammary gland development and maintenance. Nature *479*, 189–193.

Walters, M.S., Gomi, K., Ashbridge, B., Moore, M.A.S., Arbelaez, V., Heldrich, J., Ding, B.-S., Rafii, S., Staudt, M.R., and Crystal, R.G. (2013). Generation of a human airway epithelium derived basal cell line with multipotent differentiation capacity. Respir. Res. *14*, 135.

Wang, X., Yamamoto, Y., Wilson, L.H., Zhang, T., Howitt, B.E., Farrow, M.A., Kern, F., Ning, G., Hong, Y., Khor, C.C., et al. (2015). Cloning and variation of ground state intestinal stem cells. Nature *522*, 173–178.

Yamazaki, S., Iwama, A., Takayanagi, S., Eto, K., Ema, H., and Nakauchi, H. (2009). TGF-beta as a candidate bone marrow niche signal to induce hematopoietic stem cell hibernation. Blood *113*, 1250–1256.

Yang, A., Schweitzer, R., Sun, D., Kaghad, M., Walker, N., Bronson, R.T., Tabin, C., Sharpe, A., Caput, D., Crum, C., and McKeon, F. (1999). p63 is essential for regenerative proliferation in limb, craniofacial and epithelial development. Nature *398*, 714–718.

Yin, X., Farin, H.F., van Es, J.H., Clevers, H., Langer, R., and Karp, J.M. (2014). Niche-independent high-purity cultures of Lgr5+ intestinal stem cells and their progeny. Nat. Methods *11*, 106–112.

You, Y., and Brody, S.L. (2013). Culture and differentiation of mouse tracheal epithelial cells. Methods Mol. Biol. *945*, 123–143.

Zhao, R., Fallon, T.R., Saladi, S.V., Pardo-Saganta, A., Villoria, J., Mou, H., Vinarsky, V., Gonzalez-Celeiro, M., Nunna, N., Hariri, L.P., et al. (2014). Yap tunes airway epithelial size and architecture by regulating the identity, maintenance, and self-renewal of stem cells. Dev. Cell *30*, 151–165.